

Application of High-Resolution Magic-Angle Spinning NMR Spectroscopy to Define the Cell Uptake of MRI Contrast Agents

Luisella Calabi,* Goffredo Alfieri,* Luca Biondi,* Mario De Miranda,* Lino Paleari,* and Stefano Ghelli†¹

*Bracco Imaging S.p.A., Centro Ricerche Milano, via E. Folli, 50-20134 Milan, Italy; and †Spin di Stefano Ghelli, via Tamagno, 3-42048 Rubiera (RE), Italy

Received October 30, 2001; revised April 25, 2002; published online July 3, 2002

A new method, based on proton high-resolution magic-angle spinning (¹H HR-MAS) NMR spectroscopy, has been employed to study the cell uptake of magnetic resonance imaging contrast agents (MRI-CAs). The method was tested on human red blood cells (HRBC) and white blood cells (HWBC) by using three gadolinium complexes, widely used in diagnostics, Gd-BOPTA, Gd-DTPA, and Gd-DOTA, and the analogous complexes obtained by replacing Gd(III) with Dy(III), Nd(III), and Tb(III) (i.e., complexes isostructural to the ones of gadolinium but acting as shift agents). The method is based on the evaluation of the magnetic effects, line broadening, or induced lanthanide shift (LIS) caused by these complexes on NMR signals of intra- and extracellular water. Since magnetic effects are directly linked to permeability, this method is direct. In all the tests, these magnetic effects were detected for the extracellular water signal only, providing a direct proof that these complexes are not able to cross the cell membrane. Line broadening effects (i.e., the use of gadolinium complexes) only allow qualitative evaluations. On the contrary, LIS effects can be measured with high precision and they can be related to the concentration of the paramagnetic species in the cellular compartments. This is possible because the HR-MAS technique provides the complete elimination of bulk magnetic susceptibility (BMS) shift and the differentiation of extra- and intracellular water signals. Thus with this method, the rapid quantification of the MRI-CA amount inside and outside the cells is actually feasible. © 2002 Elsevier Science (USA)

Key Words: cell membrane permeability; HR-MAS; MRI; contrast agents; organ selectivity.

INTRODUCTION

The permeability of human cells by contrast agents, in particular magnetic resonance imaging contrast agents (MRI-CAs), is a matter of general interest, because it is closely linked to pharmacological and toxicological aspects associated with the administration of these substances to humans.

Up to now, human cell permeability to CAs has been rarely investigated, mainly due to the insufficient reliability of results. The few reports given in the literature use chemical methods which require a rigorous separation of cells from extracellular fluid, a time-consuming task not free of problems (i.e., breaking

of cells can invalidate the results). Also spectroscopic methods have been investigated, owing to their ability to work both on *in vivo* and *in vitro* systems without any manipulation of the sample. In any case, only those effects that are indirectly linked to permeability have been measured (1). In our opinion, none of these methods is able to give a completely unambiguous result, as would be seen necessary.

Several papers and reviews (2) have been published about the use of NMR spectroscopy together with paramagnetic complexes in order to quantify the concentration of metal ions inside and outside the cellular compartments by inducing a detectable difference between their intra- and extracellular NMR signals, usually isochronous. In principle, these techniques could also be used for the opposite aim, that is, to detect the presence of the paramagnetic complex in the different cellular compartments, by using the metal ion NMR signal as a probe (3). More generally, the NMR signals of all the substances which stay in both intra- and extracellular compartments can be used for this aim if they undergo magnetic effects in the proximity of a paramagnetic complex. This condition supplies the basis for a method, based on NMR spectroscopy, to detect the cell uptake of paramagnetic complexes, such as those commonly employed as a magnetic resonance imaging contrast agent (MRI-CA).

Three main methods, based on NMR spectroscopy spectra, have been employed to generate a detectable difference between the intra- and extracellular metal ion signals: (i) the relaxation method (4), which uses gadolinium complexes and salts; (ii) the shift method (5), which uses lanthanide complexes and salts; and (iii) the shift-relaxation method (6), which is a combination of the previous methods.

By using the relaxation method, Degani and co-workers affirmed that Gd(EDTA)⁻ is not able to diffuse into phosphatidylcholine vesicles (4). In this case a pulse sequence of 180°–τ–90° was employed in order to differentiate between the isochronous intra- and extracellular sodium NMR signals, putting one signal 180° out of phase with respect to the other. By this method, the intra- and extracellular sodium signals appear overlapped and show opposite phases. Moreover, the intensity of the broader signal (i.e., the signal of sodium in the near proximity of the gadolinium complex) is strongly reduced, as a consequence of the employed pulse sequence which acts upon the differences

¹ To whom correspondence should be addressed.

in the longitudinal relaxation times of the two signals. Under these conditions, it is our opinion that the precise measurement of the areas of the intra- and extracellular sodium signals is not possible and, consequently, qualitative measurements are also not possible.

The shift method is more attractive than the relaxation method because, in general, the lanthanide induced shift (LIS) can be easily measured and is directly linked to the concentrations of the paramagnetic species. Unfortunately, in compartmentalized systems, bulk magnetic susceptibility (BMS) (7–9), which does not influence the measurement of the metal ion concentration, makes this method unusable in order to detect and quantify the paramagnetic species in the different cellular compartments. In fact, LIS of the intracellular signals due to BMS can also exist even when the paramagnetic species remain in the extracellular compartment.

Finally, the shift-relaxation method, in our opinion, is a little more complicated and does not offer any meaningful improvement on the previous ones. As a consequence of these drawbacks, none of these methods has yet been applied to define the cell uptake of MRI-CAs because of their unsuitability for this purpose.

In this paper a method to define the cell uptake of MRI-CA is presented. It utilizes the shift and relaxation methods with some adjunctive expedients and hardware devices, which make the method easy to use and enables it to supply quantitative results. In particular it is based on: (i) the magic-angle spinning NMR technique (MAS-NMR) to nullify any shift due to BMS (10); (ii) the water NMR proton signal as probe; (iii) the high-resolution MAS technique (HR-MAS-NMR) in order to make the water signals sharp enough to allow the detection of very small LIS. For some kinds of cells, intra- and extracellular water proton resonances show two different and well distinguishable chemical shifts (11); (iv) the use of paramagnetic complexes, isostructural to the gadolinium ones, which produce well detectable LIS and very weak relaxation effects.

Relaxation enhancement effects only allow qualitative detection of the presence of the MRI-CA inside the cells, while LIS effects can be related to the paramagnetic complex concentration in the intra- and extracellular compartments, allowing quantitative determination of the cell uptake. The precision of the quantitative measurements is guaranteed by the absence of BMS and by the very careful control of the frequency of the observed signals, made possible by the use of external deuterium lock and reference signals.

The method was tested on human red blood cells (HRBC) and white blood cells (HWBC). Three gadolinium complexes, widely employed as MRI-CA for total body and specific applications (i.e., liver and CNS), were selected: Gd-BOPTA (12) (BOPTA = (4RS)-[4-carboxy-5,8,11-tris(carboxymethyl)-1-phenyl-2-oxa-5,8,11-triazatridecan-13-oic acid]), Gd-DTPA (DTPA = diethylenetriaminepentaacetic acid), and Gd-DOTA (DOTA = 1,4,7,10-tetraazocyclo-dodecane-*N,N',N'',N'''*-tetraacetic acid), each of them as sodium salts. Also Dy(III), Nd(III), Tb(III) complexes of BOPTA, DTPA, and DOTA—isostructural

to the ones of gadolinium (13)—were employed in order to perform experiments based on LIS.

The choice of HRBC and HWBC was promoted by the importance of these cells in MRI applications, mainly MRI-angiography (14), and by the simplicity in handling them during the tuning of the method. The water signal was preferred, to other potentially usable resonances, because of its high intensity and because water is widely present in all tissues. That offers the possibility of studying the permeability of a large number of cells and to perform measurements in a few minutes, very important in order to preserve the integrity of the cells during the measurements.

RESULTS

Figure 1a shows the region between 5.5 and 4.5 ppm of the ^1H HR-MAS NMR spectrum of packed human red blood cells

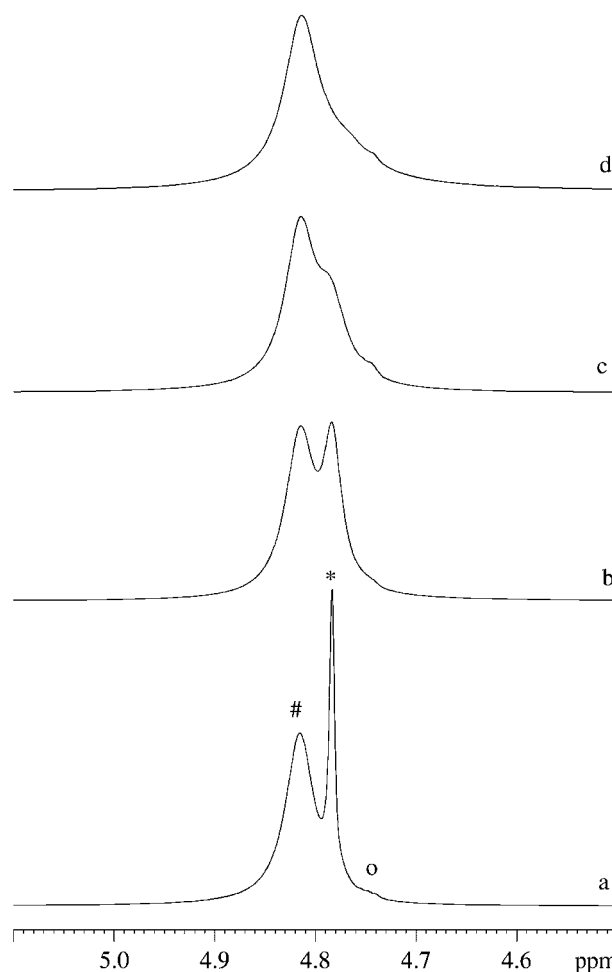


FIG. 1. (a) The 600-MHz ^1H HR-MAS NMR spectra of packed HRBC suspension in serum (RBC/serum = 80/20): #, intracellular water signal, *, extracellular water signal, o, H_2O residue of D_2O employed as the external lock signal. (b)–(d) Same sample of trace (a) but after the addition of Gd-BOPTA 0.1 M stock solution, respectively, 10–20–80 μl .

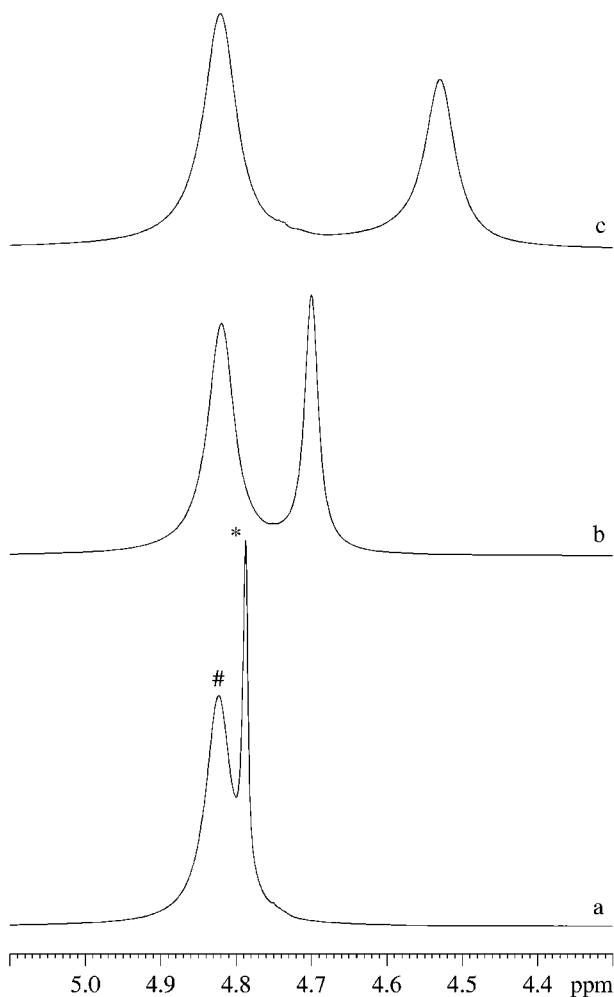


FIG. 2. (a) The 600-MHz ^1H HR-MAS NMR spectra of packed HRBC suspension in serum (RBC/serum = 80/20): #, intracellular water signal, *, extracellular water signal. (b)–(c) Same sample of trace (a) but after the addition of Dy-BOPTA 0.1 M stock solution, respectively, 20 and 80 μl .

(80% hematocrit) without water signal suppression. Two resonances appear, separated by about 19.7 Hz. The downfield shift is due to intracellular water, while the other is due to extracellular water (11). The two resonances exhibit a half-height linewidth of 17.5 and 4.6 Hz, respectively, in accordance with what was previously observed and discussed (11). This is quite a different result with respect to the usual linewidth in conventional ^1H NMR spectra, where only one resonance is detectable, with a half-height width of more than 20 Hz. Figures 1b–1d show spectra analogous to that of Fig. 1a but obtained after the addition of 10, 20, and 80 μl of Gd-BOPTA stock solution (see under Experimental). Final MRI-CA concentrations were, respectively, $0.99 \cdot 10^{-3}$, $1.96 \cdot 10^{-3}$, and $7.46 \cdot 10^{-3}$ M. The signal due to the intracellular water does not show any modification, while the extracellular water signal undergoes a clearly detectable linewidth broadening, increasing as the concentration of Gd-BOPTA increases. A small signal also appears in all the spectra, at about

4.74 ppm, due to the residue of H_2O in D_2O employed for the external lock signal (see under Experimental).

Experiments analogous to the ones reported in Fig. 1 were repeated using Dy-BOPTA instead of Gd-BOPTA. Figures 2b and 2c show, respectively, spectra acquired after additions of 20 and 80 μl of Dy-BOPTA stock solution. The extracellular water signal shows a high-field LIS which increases as the concentration of added shift reagent increases, while the intracellular water signal does not shift. Measurements performed with the addition of 320 μl of Dy-BOPTA stock solution to 1 ml of HRBC sample (100% hematocrit) (final Dy-BOPTA concentration was $24.22 \cdot 10^{-3}$ M) confirmed this behavior: the intracellular water signal did not shift while the extracellular proton water signal showed a shift of 0.76 ppm (data not shown).

Measures analogous to those shown in Fig. 2 were repeated by using Nd-BOPTA and Tb-BOPTA stock solutions (Figs. 3b and 3c), in order to prove the correctness of extrapolating the Gd-BOPTA behavior from that of Dy-BOPTA. LIS was confirmed for the extracellular water signal only, while the intracellular water signal remained unaffected. Once this relationship was

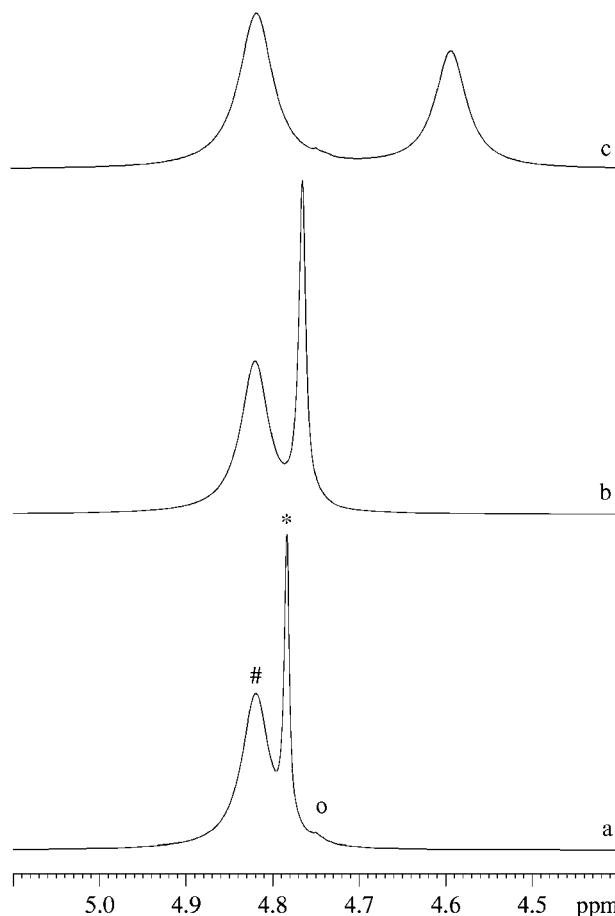


FIG. 3. (a) The 600-MHz ^1H HR-MAS NMR spectra of packed HRBC suspension in serum (RBC/serum = 80/20): #, intracellular water signal, *, extracellular water signal. (b)–(c) Same sample of trace (a) but after the addition, respectively, of 80 μl of Nd-BOPTA and Tb-BOPTA 0.1 M stock solutions.

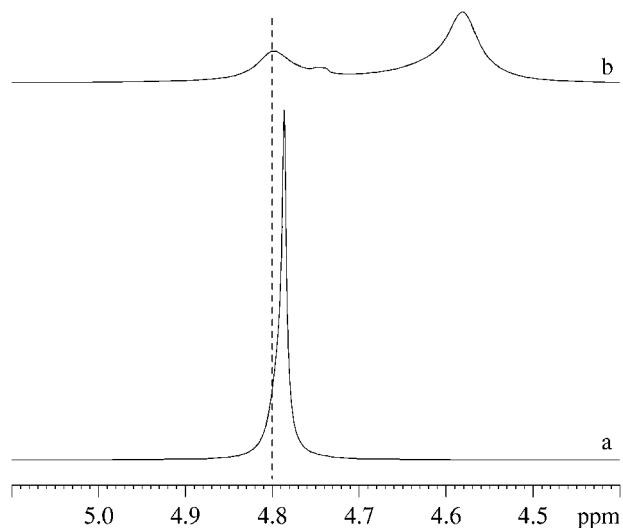


FIG. 4. (a) The 600-MHz ^1H HR-MAS NMR spectra of packed HWBC suspension in phosphate buffer solution. (b) Same sample of trace (a) but after the addition of $80\ \mu\text{l}$ of Dy-BOPTA 0.1 M stock solution.

established, for all the other experiments, dysprosium complexes were only used, because they produce the easiest detectable effects compared with other lanthanide complexes.

In Fig. 4a, the ^1H HR-MAS NMR spectrum of HWBC is shown. Contrary to HRBC, the intra- and extracellular resonances do not appear well separated, although the signal shows an asymmetry revealing the presence of two overlapped signals. The addition of Dy-BOPTA stock solution produced similar behavior to that observed for HRBC; i.e., the extracellular water signal shows a high-field LIS which increases as the concentration of added shift reagent increases, while the intracellular water signal does not shift (Fig. 4b).

To get further proof, HRBC and HWBC were fixed and then suspended in a phosphate buffer solution in order to destroy the cell membrane functionality. In these cases, the separation between intra- and extracellular water signals was lower with respect to that of no fixed cells (Figs. 5a and 5c). The addition of Dy-BOPTA stock solution produced high-field shifts of both the intra- and extracellular water signals (Fig. 5b) proving that in this case, as expected, Dy-BOPTA crosses the cellular membrane. The same behavior was observed with HWBC (Fig. 5d).

In Fig. 6, proton ^1H HR-MAS NMR spectra of HRBC after the addition of Dy-DOTA (Fig. 6b) and Dy-DTPA (Fig. 6c) stock solutions are shown. Again, the LIS is clearly detectable and it concerns the extracellular water signal only. Analogous results were obtained with HWBC.

In Fig. 7 the plots of the observed proton water LIS vs the concentrations (ρ) of Dy-BOPTA in physiological solution and in serum are shown (spectra were acquired with HR-MAS probe by using the same experimental conditions employed for HRBC and HWBC). Detectable LIS was found at very low values of ρ (Table 1). Figure 7 also reports the plots of the observed proton

TABLE 1
LIS of Proton Water Signal vs Concentration of Added Paramagnetic Complex, Observed in ^1H HR-MAS NMR Spectra Acquired at 600 MHz

ρ	LIS (Hz) ●	LIS (Hz) ○	LIS (Hz) ▼	LIS (Hz) ▽
0,00	0.00	0.00	0.00	0.00
0,05	-0.49	-0.45	-0.55	-0.30
0,10	-1.00	-1.19	-2.02	-0.37
0,50	-3.25	-2.72	-3.85	-2.20
1,00	-3.46	-4.08	-8.07	-4.77
2,00	-5.39	-10.57	-18.34	-9.54
4,00	-18.47	-21.31	-39.99	-20.18
8,00	-36.45	-45.51	-80.52	-40.17
16,00	-79.38	-92.12	-161.95	-81.43

Note. ●, Dy-BOPTA in physiologic solution; ○, Dy-BOPTA in serum; ▼, Dy-DOTA in serum; ▽, Dy-DTPA in serum; ρ = mM concentration.

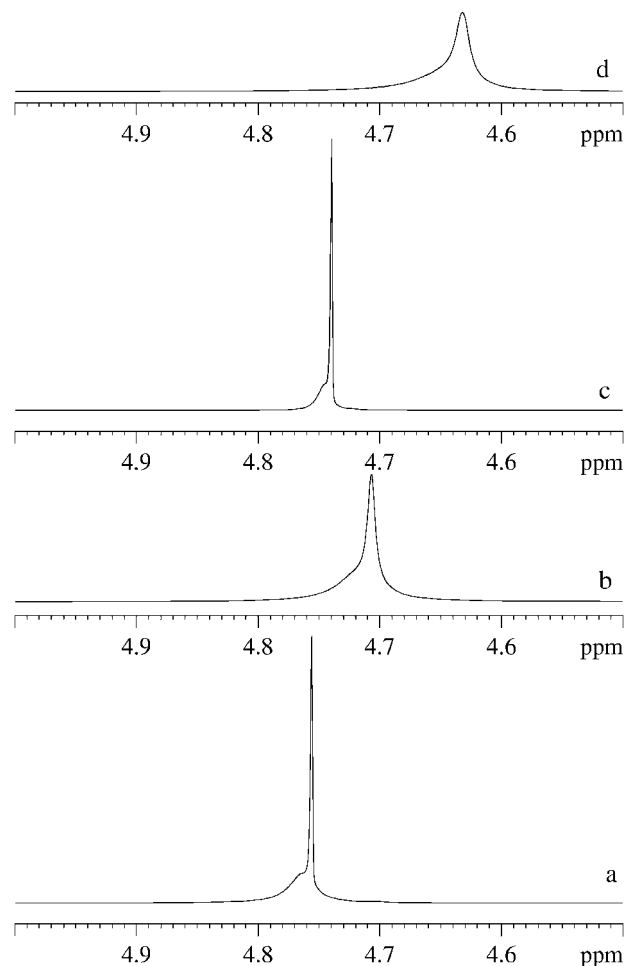


FIG. 5. (a) The 600-MHz ^1H HR-MAS NMR spectra of packed HRBC fixed and then suspended in phosphate buffer solution. (b) Same sample of trace (a) but after the addition of $80\ \mu\text{l}$ of Dy-BOPTA 0.1 M stock solution. (c) The 600-MHz ^1H HR-MAS NMR spectra of packed HWBC fixed and then suspended in phosphate buffer solution. (d) Same sample of trace (c) but after the addition of $80\ \mu\text{l}$ of Dy-BOPTA 0.1 M stock solution.

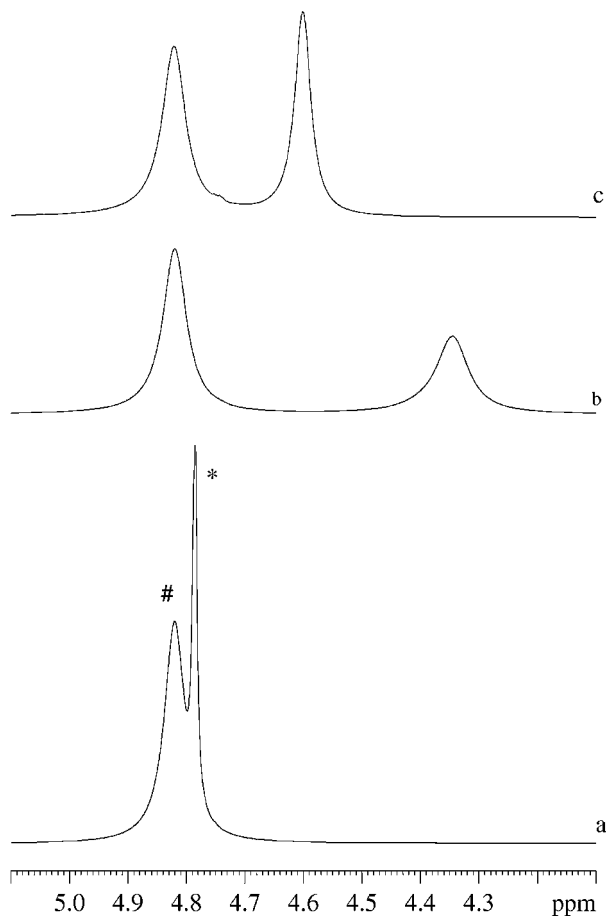


FIG. 6. (a) The 600-MHz ^1H HR-MAS NMR spectra of packed human blood cell suspension in serum (RBC/serum = 80/20): #, intracellular water signal, *, extracellular water signal. (b)–(c) Same sample of trace (a) but after the addition, respectively, of 80 μl of Dy-DOTA and Dy-DTPA 0.1 M stock solutions.

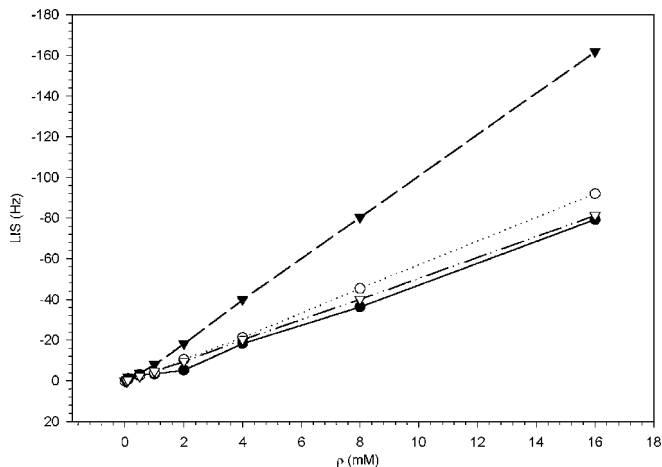


FIG. 7. Plots of observed LIS of proton water signal vs concentration ρ (mM) of added paramagnetic complex. Spectra were acquired at 600 MHz by HR-MAS technique. ●, Dy-BOPTA in physiologic solution; ○, Dy-BOPTA in serum; ▼, Dy-DOTA in serum; ▽, Dy-DTPA in serum.

water LIS vs the concentrations of Dy-DTPA and Dy-DOTA in serum.

For completeness, experiments were also attempted using a conventional 5-mm HR probe and cylindrical or spherical NMR tubes. With cylindrical NMR tubes, the addition of Dy-BOPTA to HRBC induced a strong shift of extracellular water signal but also the intracellular water signal showed a remarkable shift, due to BMS (data not shown). At last, with spherical NMR tubes, which nullify any BMS effects (15), the magnetic field homogeneity was never good enough to detect small shift effects.

DISCUSSION

Results reported in Figs. 1–4, 6 show that Gd(III), Dy(III), Nd(III), and Tb(III) complexes with BOPTA and Dy(III) complexes with DTPA and DOTA, when added to suspensions of HRBC and HWBC, produce detectable effects (line broadening or LIS) only on the extracellular water signal while the intracellular water signal does not show modifications. Under the experimental conditions employed in the tests, i.e., utilization of the MAS technique, lock signal, and reference signal, these results prove that all these paramagnetic complexes stay in the extracellular compartment only. In fact, relaxation effects are shortrange (i.e., only the signal of the water in the close proximity of the gadolinium complex can undergo a line broadening) and only diamagnetic, contact, and pseudocontact shifts can contribute to LIS (i.e., LIS effects can only exist for the water molecules which stay in the same cellular compartment of the paramagnetic species).

This assertion is true within the detection limits of the measured effects. Spectra reported in Figs. 1–3 show that LIS is more reliable with respect to the line broadening. In fact, line broadening is difficult to evaluate in the cases of small changes of the linewidth and when both intra- and extracellular water resonances broaden, as it occurs when there is a partial penetration of the CA in the intracellular compartment. Consequently, the measure of this effect can only furnish qualitative results. On the contrary, the LIS is very easy to detect and can allow, in principle, quantitative measurements because it can be related to the concentration ρ of the paramagnetic species. Consequently, the detection limits of LIS can also be evaluated and the quantitative determination of the cell uptake of the paramagnetic complexes, isostructural to the ones of gadolinium, can be achieved.

The detection limits of LIS can be evaluated by data reported in Table 1 and Fig. 7 which show that Dy-BOPTA concentrations greater than 0.5 mM induce LIS greater than 2 Hz in physiological solution and in serum (i.e., the extra-cellular fluid in our experiments). As it is shown in Fig. 8, where the ^1H HR-MAS NMR spectrum of packed HRBC is plotted three times with a shift of 2 Hz between adjacent traces, a shift of 2 Hz is well detectable for both extra- and intracellular water signals. Since it is reasonable that water molecules in the extra- and intracellular fluids behave in a very similar way, with respect to paramagnetic complexes, it is possible to affirm that, within a

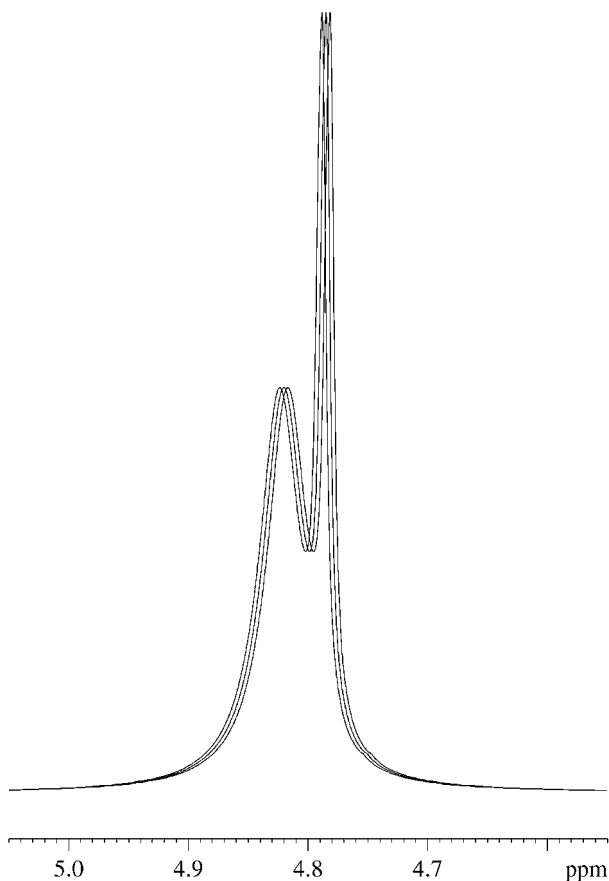


FIG. 8. The 600-MHz ^1H HR-MAS NMR spectra of packed human blood cell suspension in serum (RBC/serum = 80/20) plotted three times with a shift of 2 Hz between adjacent traces.

detection limit equivalent to a concentration of 0.5 mM (i.e., 2-Hz shift), Dy-BOPTA does not cross the HRBC membrane because, in the opposite case, it should have induced a detectable LIS for the intracellular water signals.

The hypothesis that water in the extra- and intracellular fluids should behave in a very similar way is almost reasonable because, at low concentrations of Dy-BOPTA, water does not show relevant differences in LIS between physiological solution and serum (Fig. 7), in spite of the big difference in the composition of these two media. Furthermore, it is also important to observe that it is very difficult to obtain plots, like those shown in Fig. 7, for water in the intracellular fluid because of the difficulty in getting samples of this fluid alone. In fact, the breaking of the cellular membrane cannot be achieved by using the traditional method which requires one to put the cells in a hypotonic solution. Other methods cannot be used either. For instance, the ultrasonic wave treatment strongly modifies the cellular fluid by heating.

In the absence of detectable shift of the intracellular water signal, it is possible to consider an overestimated Dy-BOPTA concentration in the intracellular compartment equal to 0.5 mM

(i.e., the detection limit). In this hypothesis, considering an overestimated intracellular fluid volume of 0.8 ml (80% hematocrit), it results in an underestimated gradient of concentration, between extra- and intracellular compartments, of about 54.3 : 1, when 80 μl of Dy-BOPTA 0.1 M stock solution are added. This gradient of concentration, although underestimated, is high enough to affirm that Dy-BOPTA does not cross the HRBC membrane because, in the case of permeability, a much lower gradient would be expected. These calculations, performed for the sample obtained by addition of 320 μl of Dy-BOPTA 0.1 M stock solution to 1 ml of HRBC sample (100% hematocrit), give an underestimated gradient of concentration, between extra- and intracellular compartments, of about 197 : 1. This result quantitatively confirms that Dy-BOPTA does not cross the HRBC.

Results for Dy-DTPA and Dy-DOTA are similar to those of Dy-BOPTA, as shown in Figs. 6 and 7 and in Table 1. A detection limit equivalent to a concentration of 0.5 mM was found and, by using calculations similar to those reported for Dy-BOPTA, it is possible to affirm that these two complexes do not cross the cellular membrane of HRBC. Since the behavior in HWBC was proved to be analogous with that in HRBC (Fig. 4), and since it was also proved that Dy-BOPTA behaves like Gd(III)-BOPTA, the conclusions found for HRBC and Dy(III) complexes of BOPTA, DTPA, and DOTA can be extended to HWBC and to Gd(III) complexes of BOPTA, DTPA, and DOTA.

It is noteworthy that in all the shown spectra the extracellular water signal increases in area with respect to the intracellular signal, as the amount of paramagnetic complex solution is increased. This effect is due to the increment of the extracellular water due to the addition of the paramagnetic complex stock solution but that does not modify in any way the quantitative measurements because LIS gives directly the concentrations by the plots reported in Fig. 7. Moreover, in the case of partial penetration of the CA in the intracellular compartment, calculations similar to those just reported can furnish a quantitative estimation of the gradient of concentration between extra- and intracellular compartments.

Experiments performed by using HRBC and HWBC, whose membrane functionality was deliberately destroyed (Fig. 5), have furnished a clear picture of the situation which can occur when the paramagnetic complex crosses the cellular membrane, giving further proof that intra- and extracellular proton water resonances act as sensors of the cellular compartment where the paramagnetic complex stays.

It is also noteworthy to comment on the differences existing among spectra obtained using a conventional 5-mm HR probe (i.e., cylindrical and spherical NMR tubes), a MAS probe, and a HR-MAS probe. In the first case (conventional 5-mm HR probe) methods to evaluate the BMS contribution to LIS are reported in the literature (15–18) but these procedures are complex and, in our opinion, not completely satisfying, especially for detecting small shifts. MAS probe eliminates BMS but the absence of the lock channel does not allow one to obtain optimal shimming conditions and a magnetic field stable enough to get very

sharp signals. In fact, only a water proton signal is detectable in HRBC and HWBC suspensions. Therefore the sensitivity to detect small LIS is smaller with respect to the HR-MAS probe. Of course, within higher detection limits, MAS probes could also be used.

Finally, it is noticeable that the literature includes papers based on HR-MAS NMR on human prostate tissue (19), dystrophic cardiac tissue (20), intact kidney samples (21), glioblastoma multiforme cells (22), and brain tumor tissue (23). All of these allow one to suppose that this method can be applicable to other living systems and, in principle, to any type of cells and tissues. Probably, different types of cells or tissues may show different behavior, i.e., different chemical shift separation between intra- and extracellular water and different lineshapes. The spectra of HRBC and HWBC furnish an example of that: intra- and extracellular water resonances are well separated in HRBC while in HWBC they are partially overlapped (Fig. 4). The reasons for this different behavior is not known but that does not limit, in general, the applicability of the method. Different types of cells or tissues could also show different limits of detectable LIS which could determine different limits of sensitivity of the determination of the cell uptake. The limit of detectable LIS can also depend on the nature of the paramagnetic complex.

The method is applicable, in principle, to any molecule and metal ion which shares itself between intra- and extracellular compartments.

CONCLUSION

The ^1H HR-MAS NMR spectroscopy method proposed here allows for an easy, fast, direct, and quantitative determination of the amount of MRI-CA inside and outside the cells, by means of the differentiation of intra- and extracellular water signals and the complete elimination of bulk magnetic susceptibility shifts.

Because cells are in no way pretreated, the method is very fast, free of any sample manipulation and, in principle, applicable to any type of cells and tissues. That means that the method makes it easier to carry out a variety of studies on MRI-CA organ selectivity and toxicity and allows the deepening of this matter, very relevant for the development and the improvement of MRI-CA. Moreover, due to the feasibility of the measurements and the ubiquity of water in living systems, this new HR-MAS approach offers the possibility of studying the permeability of a large number of cells by a wide typology of MRI CAs.

Lanthanide complexes would be better than gadolinium complexes because the former give a better picture of the phenomena, since shift effects are easier to detect and to quantify than relaxation effects (line broadening).

In the present study it is also proved that HRBC and HWBC have no permeability towards Gd-BOPTA, Gd-DTPA, and Gd-DOTA, useful information for the development of new applications of these MRI-CA. Studies on other cells, other MRI-CA, and other NMR signals which can act as a probe of the cellular compartments are in progress.

EXPERIMENTAL

Centrifugation. The employed centrifuge was Heraeus Sepatech Omnifuge 2 ORS, rotor model 3360; centrifugation was done at 2109 g (equivalent to 3500 rpm) at 4°C for 15 minutes, unless noted otherwise; condition changes noted only when necessary.

Living HRBC preparation. Human blood (to which sodium citrate as an anticoagulant was added) was centrifuged. After that, HRBC pellets were separated from serum and white cell interface, taking care to obtain a solution of red cells free of white cells. HRBC and pure serum were then put together again, with a ratio of 4 : 1 (80% hematocrit).

Living HWBC preparation. Human blood (to which sodium citrate as an anticoagulant was added) was centrifuged at 248 g (equivalent to 1200 rpm). After that, PRP (platelet rich plasma) was separated and the sediment was suspended again in phosphate buffer and centrifuged. The buffy coat (HWBC and HRBC) was collected, suspended in the usual buffer (up to the original volume), added with Emosol (tenth part of the total volume) and left for 10 minutes; Emosol breaks the HRBC membrane. After this time, the supernatant liquid was removed, the whole washing repeated, and the HWBC were ready.

Fixed HWBC and HRBC preparation. Living HRBC (or HWBC), as previously prepared, were dissolved to the initial volume with a phosphate buffer (Soerensen 0.1 M pH = 7.4) and centrifuged; then the buffer was removed and this washing was repeated three times. Then, 400 μl of HRBC (or HWBC) were suspended in 588 μl of the previous buffer to which was added 12 μl of glutaraldehyde (25% aqueous solution) and shaken for 20 h. After this time, HWBC were washed with distilled water (10 times in volume) and centrifuged for only 1 minute, repeating this treatment three times.

Lanthanide complexes. Lanthanide complexes were prepared according to Ref. (12) and related patents.

Samples containing lanthanide complexes. All the samples were obtained by addition of definite amounts of 0.1 M stock solution of lanthanide complexes to 1 ml of HRBC or HWBC samples, prepared as previously described. All the concentrations reported in the text refer to the whole sample (i.e., a volume equal to 1 ml plus the microliters of added stock solution).

Calculation of the gradient of concentration. Intracellular fluid volume = 800 μl (80% hematocrit); extracellular fluid volume = 200 μl + 80 μl (volume of the added lanthanide complex 0.1 M stock solution to 1 ml of HRBC); added lanthanide complex = 80 μl · 0.1 M = 8 μmole ; lanthanide complex in the intracellular, considering a detection limit of 0.5 M = 0.5 M · 800 μl = 0.4 μmole ; lanthanide complex in the extracellular = 8 μmole - 0.4 μmole = 7.6 μmole ; concentration of lanthanide complex in the extracellular = 7.6 μmole / 280 μl = 27.14 mM; concentration gradient, 27.14 M / 0.5 M = 54.28 : 1. Really, the concentration of lanthanide complex in the extracellular was less than the detection limit. Therefore the

calculated concentration gradient was underestimated. Moreover, the volumes of intracellular and extracellular fluid were less than 800 μl because not all the volume of the RBC was due to water. That means that the calculated concentration gradient was further underestimated.

NMR spectra. Proton HR-MAS NMR spectra were acquired on a Bruker Avance 600 spectrometer operating at the frequency of 600.13 MHz. A Bruker HR-MAS 4-mm rotor double bearing probehead, equipped with a deuterium lock channel and with double coils designed for C-13/H-1 inverse detection, were employed. Experimental conditions were spectral width = 24,000 Hz (about 40 ppm); time domain size = 64 K data points; number of scans = 128; recycle delay = 1 s, spinning rate = 3500 Hz; Fourier Transform without application of window functions on the FID. Spinning rate was limited to 3500 Hz to avoid cell disruption.

In order to have an external lock signal in such a way as to get a high stability and reproducibility of the frequency between the different spectra, rotors with spherical insert and a double cap were employed; a small amount of D_2O was always put in the small space between the inner compartment (shut by a screw), which contained the sample, and the external cap which shut the rotor. All spectra were acquired at the temperature of 25 °C. Shimming was performed only once, on the first sample of each series.

REFERENCES

1. N. Zaplatin, K. A. Baker, and F. W. Kleinhaus, Effectiveness and toxicity of several DTPA broadening agents for biological ESR spectroscopy, *J. Magn. Res. B* **110**, 249–254 (1996).
2. S. K. Miller and G. A. Elgavish, Shift-reagent-aided ^{23}Na NMR spectroscopy in cellular, tissue, and whole-organ systems, *Biol. Magn. Reson.* **11**, 159–240 (1992).
3. J. A. Balschi, J. A. Bittl, C. S. Springer, and J. S. Ingwall, ^{31}P and ^{23}Na NMR spectroscopy of normal and ischemic rat skeletal muscle: Use of a shift reagents in vivo, *NMR Biomed.* **3**, 47–58 (1990).
4. H. Degani and G. A. Elgavish, Ionic permeabilities of membranes, *FEBS Lett.* **90**(2), 357–360 (1978).
5. R. K. Gupta and P. Gupta, Direct observation of resolved resonances from intra- and extracellular sodium-23 ions in NMR studies of intact cells and tissues using dysprosium(III)tripolyphosphate as paramagnetic shift reagent, *J. Magn. Reson.* **47**, 344–350 (1982).
6. S. K. Miller, W. J. Chu, G. M. Pohost, and G. A. Elgavish, Improvement of spectral resolution in shift-reagent-aided ^{23}Na NMR spectroscopy in the isolated perfused rat heart system, *Magn. Reson. Med.* **20**, 184–195 (1991).
7. D. H. Live and S. I. Chan, Bulk susceptibility corrections in nuclear magnetic resonance experiment using superconducting solenoid, *Anal. Chem.* **42**(7), 791–792 (1970).
8. I. Pályka, W. Huang, and C. S. Springer, Jr., The effects of bulk magnetic susceptibility in NMR, *Bull. Magn. Reson.* **17**, 46–53 (1995).
9. Y. Shachar-Hill, D. E. Befroy, P. E. Pfeffer, and R. G. Ratcliffe, Using bulk magnetic susceptibility to resolve internal and external signals in the NMR spectra of plant tissues, *J. Magn. Reson.* **127**, 17–25 (1997).
10. C. S. Springer, Jr., Physicochemical principles influencing magnetopharmaceuticals, in “NMR in Physiology and Biomedicine” (R. J. Gillies, Ed.), pp. 75–99, Academic Press, Orlando (1994).
11. E. Humpfer, M. Spraul, A. W. Nicholson, J. K. Nicholson, and J. C. Lindon, Direct observation of resolved intracellular and extracellular water signals in intact human red blood cells using ^1H MAS NMR spectroscopy, *Magn. Reson. Med.* **38**, 334–336 (1997).
12. F. Uggeri, S. Aime, P. L. Anelli, M. Botta, M. Brocchetta, C. de Haen, G. Ermondi, M. Grandi, and P. Paoli, Novel contrast agent for magnetic resonance imaging: Synthesis and characterization of the ligand BOPTA and its Ln(III) complexes (Ln = Gd, La, Lu). X-ray structure of disodium (TPS-9-145337286-C-S)-[4-carboxy-5,8,11-tris(carboxymethyl)-1-phenyl-2-oxa-5,8,11-triazatridecan-13-oato(5-)]gadolinolate(2-) in a mixture with its enantiomer, *Inorg. Chem.* **34**, 633–642 (1995).
13. R. Turner and P. Keller, Angiography and perfusion measurements by NMR, *Prog. NMR Spectrosc.* **22**, 93–133 (1991).
14. L. Calabi and L. Paleari, private report.
15. S. C.-K. Chu, Y. Xu, J. A. Balschi, and C. S. Springer, Jr., Bulk magnetic susceptibility in NMR shift studies of compartmentalized samples: Use of paramagnetic reagents, *Magn. Reson. Med.* **13**, 239–262 (1990).
16. M. S. Albert, W. Huang, J.-H. Lee, J. A. Balschi, and C. S. Springer, Jr., Aqueous shift reagents for high-resolution cation NMR, VI, *NMR Biomed.* **6**, 7–20 (1993).
17. S. Fossheim, K. E. Kellar, A. K. Fahlvik, and J. Klaveness, Low-molecular weight lanthanide contrast agents: Evaluation of the susceptibility and dipolar effects in red blood cell suspensions, *Magn. Reson. Imag.* **15**(2), 193–202 (1997).
18. M. A. Brown, T. T. Stenzel, A. A. Ribeiro, B. P. Drayer, and L. D. Spicer, NMR studies of combined lanthanide shift and relaxation agents for differential characterization of ^{23}Na in a two-compartment model system, *Magn. Reson. Med.* **3**, 289–295 (1986).
19. L. L. Cheng, C. Wu, M. R. Smith, and R. G. Gonzalez, Non-destructive quantitation of spermine in human prostate tissue samples using HRMAS ^1H NMR spectroscopy at 9.4 T, *FEBS Lett.* **494**(1–2), 112–116 (2001).
20. J. L. Griffin, H. J. Williams, E. Sang, and J. K. Nicholson, Abnormal lipid profile of dystrophic cardiac tissue as demonstrated by one- and two-dimensional magic-angle spinning ^1H NMR spectroscopy, *Magn. Reson. Med.* **46**(2), 249–255 (2001).
21. J. L. Griffin, L. A. Walker, S. Garrod, E. Holmes, R. F. Shore, and J. K. Nicholson, NMR spectroscopy based metabolomic studies on the comparative biochemistry of the kidney and urine of the bank vole (*Clethrionomys glareolus*), wood mouse (*Apodemus sylvaticus*), white toothed shrew (*Crocidura suaveolens*) and the laboratory rat, *Comp. Biochem. Phys. Biochem. Mol. Biol.* **127**(3), 357–367 (2000).
22. L. L. Cheng, D. C. Anthony, A. R. Comite, P. M. Black, A. A. Tzika, and R. G. Gonzalez, Quantification of microheterogeneity in glioblastoma multiforme with ex vivo high-resolution magic-angle spinning (HRMAS) proton magnetic resonance spectroscopy, *Neuro-oncol.* **2**(2), 87–95 (2000).
23. L. L. Cheng, I. W. Chang, D. N. Louis, and R. G. Gonzalez, Correlation of high-resolution magic angle spinning proton magnetic resonance spectroscopy with histopathology of intact human brain tumor specimens, *Cancer Res.* **58**(9), 1825–1832 (1998).